Improvement of Lidar Data Accuracy Using Lidar-Specific Ground Targets

[THIS PAPER WAS THE WINNER OF THE 2005 BAE SYSTEMS AWARD GIVEN AT THE ASPRS 2005 ANNUAL CONFERENCE]

Nora Csanyi and Charles K. Toth

Abstract

With recent advances of lidar technology, the accuracy potential of lidar data has significantly improved. State-of-the-art lidar systems can achieve 2 to 3 cm ranging accuracy under ideal conditions, which is the accuracy level required by engineering scale mapping. However, this is also the accuracy range that cannot be realized by routine navigation-based direct sensor platform orientation. Furthermore, lidar systems are highly integrated multi-sensor systems, and the various components, as well as their spatial relationships, introduce different errors that can degrade the lidar data accuracy. Even after careful system calibration, including individual sensor calibration and sensors intra-calibration, certain errors in the collected data can still be present. These errors are usually dominated by navigation errors and cannot be totally eliminated without introducing absolute control information into the lidar data. Therefore, to support applications that require extremely high, engineering scale mapping accuracy, such as transportation corridor mapping, we propose the use of lidar-specific ground targets. Simulations were performed to determine the most advantageous lidar target design and targets were fabricated based upon the simulation results. To investigate the potential of using control targets for lidar data refinement, test flights were carried out with different flight parameters and target distributions. This paper provides a description of the optimal lidar target design, the target identification algorithm, and a detailed performance analysis, including the investigation of the achievable lidar data accuracy improvement using lidar-specific ground control targets in the case of various target distributions and flight parameters.

Introduction

Lidar systems have advanced considerably in recent years. In particular, the pulse rate frequency has increased significantly, the ranging accuracy has improved, and the availability of intensity signal has become common (Toth, 2004). These developments have resulted in better data quality in terms of higher point density and better accuracy, which, in turn, further widened the already broad application field of laser scanning (Renslow, 2005). For example, the centimeter-level range measurement accuracy could, in theory, support engineering scale mapping for the first time. However, this accuracy range can be achieved only for specific landscapes with good reflective characteristics and simple geometric features. Highway corridors contain mostly man-made objects with flat smooth surfaces and near-uniform reflectivity, and are usually free of vegetation thus holding the potential that the laser ranging accuracy can be approached. Of course, not all applications demand such a high accuracy. The difficulty of achieving centimeter-level accuracy, however, goes beyond laser ranging accuracy and landscape dependency, as there are many other factors in the error budget of an airborne lidar system.

Lidar systems are complex multi-sensory systems and incorporate at least three main sensors: GPS and INS navigation sensors, and the laser-scanning device. Furthermore, there is a moving component with the usual problems of position encoding, wear, and mechanical hysteresis that can further degrade the accuracy of the acquired lidar data. In general, the errors in laser scanning data can come from individual sensor calibration or measurement errors, lack of synchronization, or misalignment between the different sensors. Baltsavias (1999) presents an overview of basic relations and error formulae concerning airborne laser scanning. Even after careful system calibration, some errors could be present in the data, and navigation errors usually dominate. The errors become evident as discrepancies between overlapping strips and at ground control surfaces. Most of the systematic errors can be corrected by strip adjustment (with or without ground control) by eliminating the discrepancies between overlapping lidar strips. In the last few years, various strip adjustment methods have been developed.

Several strip adjustment methods minimize only the vertical discrepancies between overlapping strips or between strips and horizontal control surfaces. These strip adjustments can be referred as one-dimensional strip adjustment methods (Crombaghs *et al.*, 2000; Kager and Kraus, 2001). Tie or absolute control features used for this adjustment are flat horizontal surfaces. The problem with this kind of adjustment is that existing planimetric errors are likely to remain in the data. Vosselman and Maas (2001) have shown

Nora Csanyi is with The Ohio State University, Department of Civil and Environmental Engineering and Geodetic Science, 2070 Neil Avenue, Columbus, OH 43210 and The Center for Mapping, 1216 Kinnear Road, Columbus, OH 43212 (nora@cfm.ohio-state.edu).

Charles K. Toth is with The Ohio State University, The Center for Mapping, 1216 Kinnear Road, Columbus, OH 43212 (toth@cfm.ohio-state.edu).

Photogrammetric Engineering & Remote Sensing
Vol. 73, No. 4, April 2007, pp. 385–396.

0099-1112/07/7304–0385/$3.00/0

that systematic planimetric errors are often much more significant than vertical errors in lidar data, and therefore, a three-dimensional strip adjustment is the desirable solution minimizing the three-dimensional discrepancies between overlapping strips and at control points. A number of three-dimensional strip adjustment methods have been published. Kilian (1996) presents a method of transforming overlapping lidar strips to make them coincide with each other using control and tie points in a way similar to photogrammetric block adjustment. For each strip three offset, three rotation, and six time-dependent drift parameters are determined. Burman (2002) treats the discrepancies between overlapping strips as positioning and orientation errors with special attention given to the alignment error between the INS and laser scanner. Filin (2003) presents a similar method for recovering the systematic errors; the method is based on constraining the position of the laser points to the surface from which it was reflected. Toth *et al.* (2002) presents a method that tries to make overlapping strips coincide with the primary objective of recovering the boresight misalignment between the IMU and laser sensor.

One of the major difficulties of these strip adjustment methods is that due to the characteristics of lidar data, the determination of three-dimensional discrepancies between overlapping lidar strips or lidar strip and control information is not trivial. In contrast to traditional photogrammetry, establishing point correspondence between different lidar strips or lidar strip and control information is practically impossible, and therefore, area or feature-based, rather than point-based algorithms have to be used. Various methods have been published for the measurement of strip offsets. One possible approach is to interpolate the lidar data to regular grid and perform a least-squares matching between the two corresponding surface patches to determine the offsets between them (Behan, 2000). In order to be able to determine planimetric offsets in the data, height variations are required. Ideally, smooth rolling surfaces with surface normals pointing in three different directions are needed. Unfortunately, the number of such locations in a dataset is usually small. Therefore, building roofs and building corners are typically used to determine three-dimensional offsets in the data. The problem with this is that due to the interpolation to grid, the determined offset values can be significantly biased (Maas, 2000; Vosselman, 2002) and the accuracy of the determined position of such points depends a lot on the actual scan direction. One solution for this problem is presented by Maas (2000) who formulates least-squares matching of height data in a TIN structure, thereby improving the accuracy of the determined offsets. In some cases, it is not possible to find locations in the height data that are suitable to determine three-dimensional offsets between the strips. For example, horizontal planes only provide height offset information. In such cases intensity data could help to determine planimetric discrepancies. Maas (2001) describes the extension of the TIN-based matching technique using reflectance data (lidar intensity data) to replace surface height texture for the determination of planimetric strip offsets in flat areas with sufficient reflectance texture. Vosselman (2002) offers another solution, a type of a feature-based matching to avoid interpolation of the data, using linear features, gable roofs, and ditches modeled by analytical functions that can provide accurate offset determination.

Most of the strip adjustment methods only require relative control information (tie points) with absolute control information being optional. However, for applications requiring centimeter-level accuracy, absolute control information is essential, since eliminating the relative discrepancies between overlapping strips does not provide an absolute check of the dataset. Ground control information can be used in the strip adjustment process or after strip adjustment to correct the remaining absolute errors in the corrected strips. Many times following the strip adjustment, a horizontal surface with known elevation is used to correct remaining vertical shifts in the data. However, absolute errors can be more complex than just a vertical shift; therefore, three-dimensional ground control information is desired, such as, for example, buildings, or known roof structures. Unfortunately, this type of control information is not always available in the surveyed area. Furthermore, due to the above-mentioned problems, the identification of distinct points of buildings and roof structures in lidar data can result in a biased position, which could affect the accuracy of the corrected lidar data. Therefore, for applications with high accuracy requirements, such as transportation corridor mapping, well-defined, lidar-specific ground control targets are necessary.

Since the use of lidar-specific ground control targets represents a novel idea, not yet explored in practice, simulations were performed to determine the most favorable lidar-target design. Parameters included optimal target size, shape, signal response, coating pattern, and methods to accurately determine the three-dimensional target position in the lidar dataset. The first section of the paper provides a summary of the optimal target design, and then test results based on two test flights are presented, providing a detailed performance analysis on the achievable improvements in lidar data accuracy using the lidar-specific ground control targets.

Lidar Target Design and Methodology

Target Design

In the design of the optimal lidar target, the objective was to find a design that facilitates easy identification of the target in lidar data and provides highly accurate positioning accuracy in both horizontal and vertical directions. The target positioning accuracy is crucial since it determines the lower boundary for errors in the data that can be detected and corrected based on the lidar targets. After analyzing the characteristics of lidar data, it was found that due to the different possible scan directions and different point densities in different directions, the optimal lidar target must be rotation invariant, circle-shaped, and in order to reliably identify targets in elevation data, the target should be elevated from the ground. Furthermore, since newer lidar systems are capable of measuring intensity data, automatic target identification can further be facilitated if targets have a coating that provides a substantially different reflectance than their surroundings. A target design meeting the above criteria would facilitate the automatic target identification in lidar data based on their known position and the expected maximum errors in the data.

Since the proposed lidar-specific targets are mobile targets, they are placed on the ground and surveyed before or after the airborne survey. For economical and practical reasons their size should be as small as possible. However, larger target size would allow more points falling on the target surface which could result in better accuracy of the determined target position. Therefore, to determine the optimal target size and coating pattern, extensive simulations were carried out (Csanyi and Toth, 2004). Lidar points on the target circle were simulated in the case of different assumed circle radii and different coating patterns, such as one- or two-concentric-circle designs with different signal response coatings. The achievable accuracy of the determined target positions from a lidar dataset mainly depends on the lidar point density with respect to the target size, the lidar footprint size, and the vertical accuracy of the lidar points. Therefore, the simulations were carried out with three different point densities, 0.25*0.25, 0.50*0.50, and 0.75*0.75 m (16, 4, and

1.8 pts/m^2). Lidar points were simulated according to typical planimetric and vertical accuracies, and distribution. For the simulations, 0.10 m (1 σ) vertical accuracy and 0.25 m footprint size of the lidar points were assumed. Noise was added to the vertical coordinates according to a normal distribution with a 0.10 m standard deviation, while for the planimetric coordinates uniform distribution was assumed. Because the accuracy of the determined target position depends a lot on the actual point distribution on the target circle, whether there are points near the sides of the circle or not, to assess the achievable accuracy of the determined target center position in lidar data, points were simulated multiple times and the root mean square error (RMSE) was calculated.

Based on the simulation results with different target designs, the major findings are the following: (a) as expected, the larger size produced better positioning accuracy, however, the results have shown that from about 5 pts/m^2 point density, a 1-m circle radius can already provide sufficient accuracy and further increasing the target size will not lead to significant improvements, (b) the two-concentric-circle design (the inner circle has half the radius of the outer circle) with different coatings results in significant accuracy improvements in the determined horizontal position since it provides additional geometric constraint in contrast to the one-circle design, and (c) the optimal coating pattern is a special white (high intensity return) coating for the inner circle and black (low intensity return) for the outer ring. Based on the simulation results, discussed in detail below, targets were fabricated by the Ohio Department of Transportation (ODOT) to support performance validation experiments under normal operational conditions; Plate 1 shows the optical as well as the lidar image of a target pair placed along a road.

Determining Target Positions

After the lidar points on the target circle are identified based on elevation and intensity information, the horizontal and vertical target positions are determined by separate algorithms. Since the targets are leveled, the vertical position of the target can be determined by fitting a horizontal plane to the points fallen on the target. A solution also exists for not-leveled targets, but it is not discussed here. The accuracy of the computed target height can be determined by error propagation based on the standard deviation of the vertical coordinates of the lidar points: $\sigma_{vertical\_pos} = \sigma_z/\sqrt{n}$, where n is the number of points on the target, and σ_Z is the vertical coordinate accuracy of the lidar points.

The horizontal target position is found by an algorithm similar to the generalized version of the Hough-transform (Hough, 1959 and 1962). Duda and Hart (1972) introduced first the generalized version of the Hough transform to detect curves. The search for the target center is based on the known radius of the target circle; the process finds all the possible locations of the target circle center in a grid. Considering a one-circle-design, the principle of the algorithm is the following: for a lidar point on the target circle, the circle center must be within the circle with known radius having the lidar point as center. Applying the same principle to all lidar points on the target, the intersection region of all circles around the points defines all the possible locations of the target circle center. The implementation of the algorithm uses 1-cm resolution accumulator array, and after incrementing the cell values by the point-by-point process, the cells with the highest value give all the possible locations of the target center, and finally the center of gravity of this region is accepted as the target center position. Figure 1a illustrates the accumulator array and Figure 1b depicts the fitted circle with the center location area and the center of gravity point on an example with about 5 pts/m^2 point density. The light grey patch shows all the possible locations of the circle center, the dark circles are the corresponding circle positions, and the light grey circle is the final accepted target circle position. Obviously, in the case of the two-concentric-circle design the algorithm is more complex, but the basic principle is the same. Figure 2 illustrates the advantage of the two-concentric-circle design compared to the one-circle design on two examples. The two-concentric-circle design, using intensity information, can clearly provide the horizontal center position with improved accuracy. The numbers next to the lidar points in the middle figures show the lidar intensity values; the comparison of the intensity values between the two cases clearly illustrates the relative nature of the intensity data. In our implementation, an intensity histogram-based adaptive thresholding scheme is used to separate points on the inner circle and the outer ring, marked with two different gray values in Figure 2. The standard deviations of the determined horizontal target center coordinates are noticeably smaller for the two-concentric-circle design; the actual

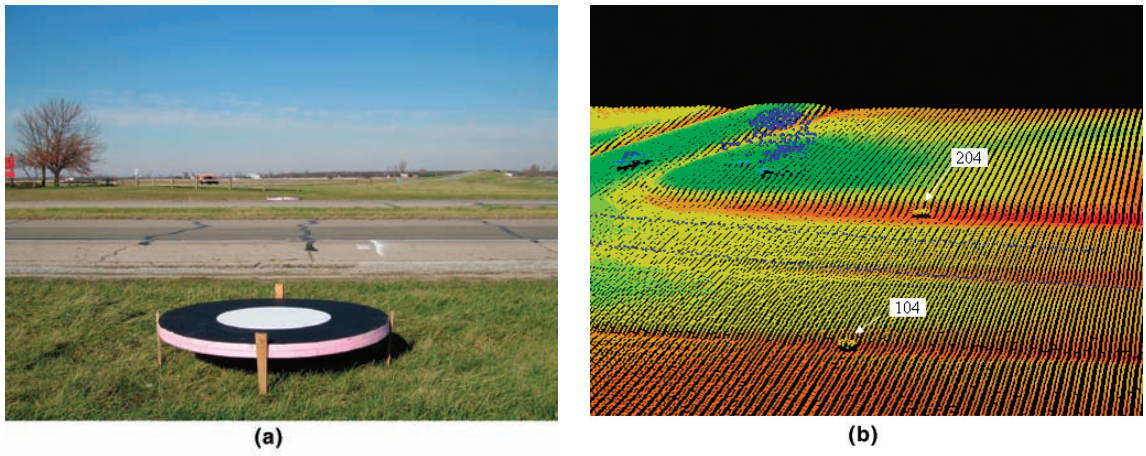

Plate 1. Lidar target pair (a) and their appearance in the lidar data (b).

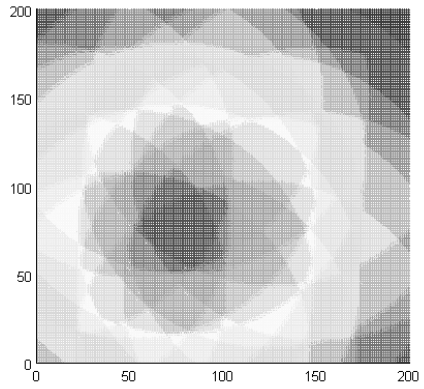

(a)

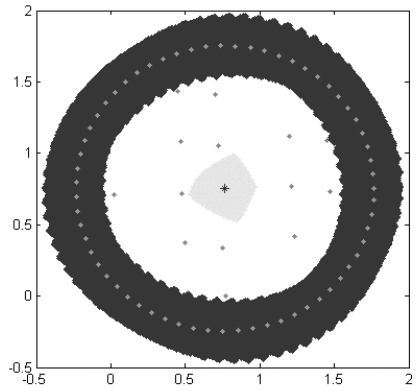

(b)

Figure 1. Accumulator array (a) and fitted circle (b). A color version of this figure is available on the ASPRS website: **www.asprs.org**.

numbers are 10 cm versus 5 cm and 14 cm versus 3 cm for Figures 2a and 2b, respectively. The vertical accuracy is invariant to the design and is 2 cm. Figure 2a can be considered as a typical case, while Figure 2b shows an extreme case where the accuracy improvement in the determined horizontal position using the two-concentric-circle design is very significant. It should be mentioned that sometimes in practice, the footprint captures intensity information from the boundary of the inner circle and outer ring, and in such cases the point in the reflectance image has mixed intensity value and cannot be included in the algorithm for the horizontal coordinate determination of the target.

Target Positioning Accuracy

The accuracy of the determined target center position defines the lower boundary for errors in the lidar data that can be detected and corrected using the lidar-specific targets. The accuracy of the target center position depends on different factors, such as lidar point density, lidar point accuracy, and the actual point distribution of the lidar points on the target. Therefore, to assess the achievable accuracy of the determined lidar target position within the lidar dataset, simulations were carried out for different lidar point densities. As an example, Table 1 contains the estimated positioning accuracies for three different lidar point densities. The lidar points were simulated assuming 10 cm vertical accuracy (1σ) and 0.25 m footprint size. The estimated values are the RMSE values calculated from numerous simulations. The results suggest that at a 4 pts/m^2 lidar point density, horizontal errors in lidar data larger than 10 cm, and vertical errors larger than 2 to 3 cm can be detected and consequently corrected using the lidar-specific targets.

Correction of Lidar Data

To automate the processing of the target-based lidar data quality check and correction, a software toolbox was developed. The main modules include the initial batch processing, which is followed by an interactive analysis, and then the actual batch correction of the lidar data takes place. In the first phase, the program without human intervention selects the target areas from the lidar strips, finds the lidar points on the targets, and determines the target positions. The extraction of the points falling on the lidar targets is accomplished in two steps. First, lidar points in the vicinity of the targets are windowed out based on the known (surveyed) target coordinates and the maximum expected errors in the lidar data. In the second step, the points not falling on targets are filtered based on vertical elevation differences, and intensity information and subsequently the remaining target candidate points are checked for geometry. Next, target positions are determined using the algorithms described in the previous section.

Once the initial data processing has been finished, the user can review the errors at target locations and, if needed, can interactively select the optimal transformation type for the lidar strip. In a similar process to blunder detection, the operator could decide whether all lidar targets should be used in the computation or exclude any targets that could be in gross error. Furthermore, extra long lidar strips could be segmented into smaller parts and then processed independently. The identified lidar targets with their lidar-derived coordinates can serve as quality control or can be used for the correction of lidar strips for any absolute error in the lidar data. If conventional lidar strip adjustment is performed the lidar targets can be used either in the adjustment or after it to correct for any remaining absolute errors in the data. The correction can be a simple vertical shift or a more complex three-dimensional transformation can be applied to the data based on the known and measured target positions. The applied transformation depends on the characteristics of the errors and the number of available targets in the dataset. If only one or two ground targets are available in the dataset, a simple vertical offset correction can be performed. If three or more targets are available, a three-dimensional similarity or a more complex transformation can be applied to the data to correct absolute errors.

Test Results

To assess the achievable accuracy improvement using the designed lidar-specific targets for lidar data refinement, data from two test flights were analyzed. The first test flight was aimed at infrastructure mapping of a transportation corridor using 15 pairs of targets placed symmetrically along the two sides of the road. The second test was a dedicated flight for investigating the target identification accuracy and the effect of targets in the improvement of lidar data accuracy for various lidar settings and target densities. Both areas were surveyed using an Optech ALTM 30/70 lidar system operated by the Ohio Department of Transportation with GPS reference stations closer than 30 km.

Test Flight 1

During the first test, several lidar strips were flown over a 23 km long section of I-90 in Ashtabula, Ohio, in both directions. The flight parameters are shown in Table 2. To support our investigation, 15 sets of lidar targets were

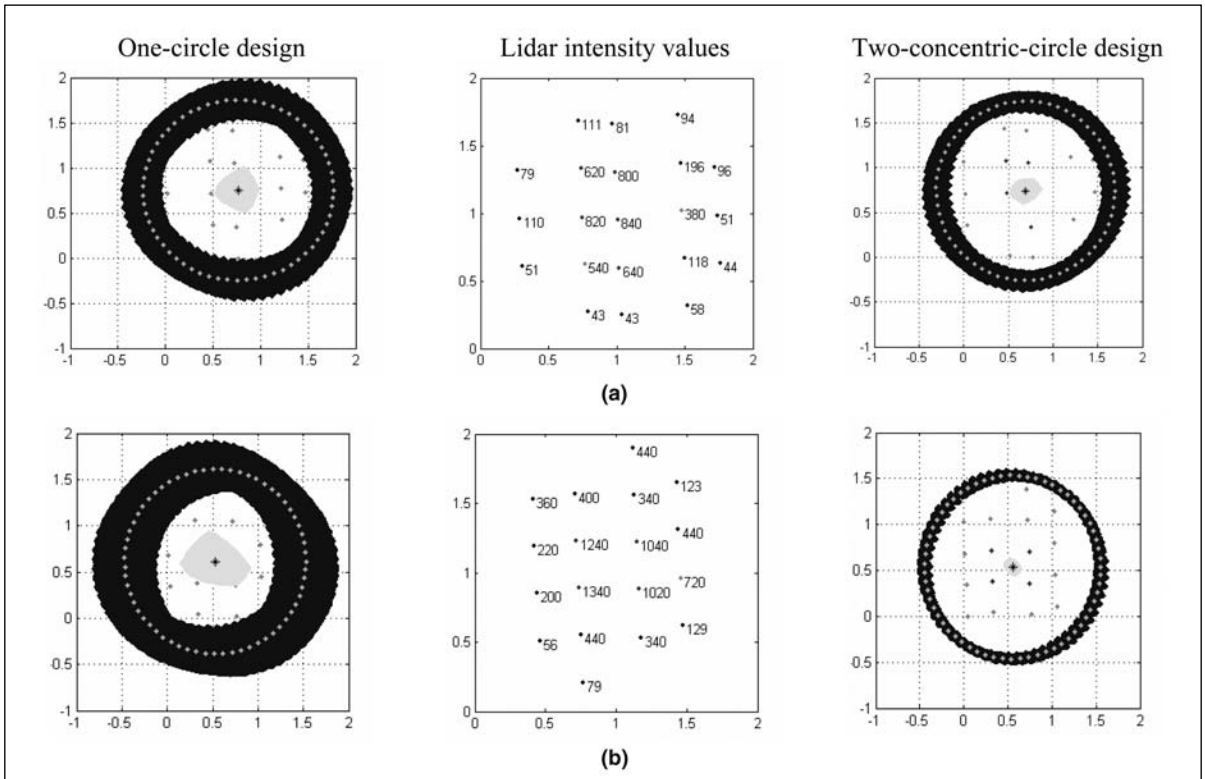

Figure 2. Advantage of the two-concentric-circle design: (a) typical case, and (b) extreme case. A color version of this figure is available on the ASPRS website: **www.asprs.org**.

TABLE 1. ESTIMATE OF POSITIONING ACCURACIES BASED ON SIMULATION RESULTS

Lidar Point Density [pts/m^2]	Lidar Point Spacing [m]	Accuracy of Horizontal Position of Target Circle [cm]	Accuracy of Vertical Position of Target Circle [cm]
16	0.25*0.25	2–3	1.3
4	0.50*0.50	5–10	2.5
1.78	0.75*0.75	10–15	4.0

placed symmetrically along the two sides of the road with an average distance of about 1,600 m between each pair of targets. The origins of the target circles were GPS-surveyed at a horizontal coordinate accuracy of approximately 2 cm and vertical accuracy of about 3 cm. Both elevation and intensity data were collected to facilitate lidar target identification.

The targets were automatically identified and positioned in all strips as discussed in the previous section, and errors found at the target locations were analyzed. Two overlapping strips flown in opposite directions were chosen for the detailed discussion here; the target locations in the two lidar strips are shown in Figure 3. The strip flown in the SW to NE direction is denoted as strip #1, and the strip flown in the opposite direction as strip #2. The strips flown along the road had a length of about 8.3 km, and ideally they contained four targets on both sides of the road. Unfortunately,

TABLE 2. ASHTABULA TEST FLIGHT PARAMETERS

Altitude (AGL)	~620 m
Scan Angle	14°
Pulse Rate	70 kHz
Scan Frequency	70 Hz
Point Density	5 pts/m^2
Footprint Size	19 cm

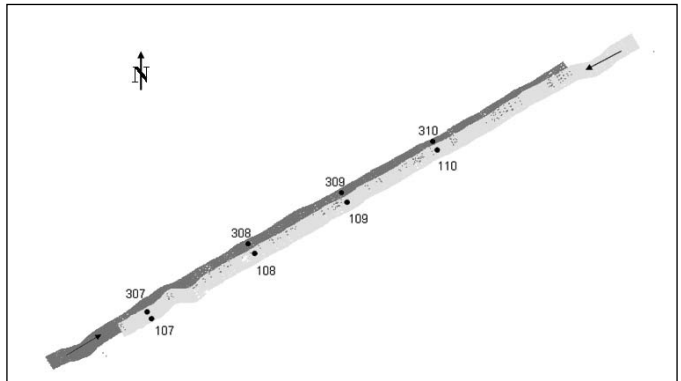

Figure 3. Lidar strips with target locations from test area 1. A color version of this figure is available on the ASPRS website: **www.asprs.org**.

the overlap of the strips fluctuated, and consequently, a couple of targets were missed from both strips.

As an example, Figures 4a and 4b depict the elevation and intensity data of a 3 m by 3 m area around target #108 in strip #1; the determined target circle position is shown in Figure 4c (note the six profiles intersecting the target surface). The intensity information creates a nice separation of the target points on the inner circle (with white coating: dark gray points in Figure 4c) and outer ring (with black coating: light gray points in Figure 4c). It should be noted that in the figure only for better visualization, the elevation and intensity values of the lidar points are interpolated to a grid, and are shown in gray-scale, but during the processing, the original lidar points (without interpolation) are used.

One important phenomenon that can have an effect on the accuracy of the determined vertical target position has to be mentioned here, namely that the reflectivity of the surface, measured in the intensity signal of the lidar points, affects the calculated range between the ground point and the laser scanner. Without intensity-based correction of the lidar data, the lidar points falling on the inner circle with white coating have higher elevation values than the lidar points that fall on the outer target ring with black coating. Lidar manufacturers provide intensity-based calibration tables for this effect, and for all the processing discussed here, the lidar data were corrected. Figure 5 illustrates lidar points on a target before the intensity-based correction of the data, showing a significant, approximately 7 cm, elevation difference between the average elevation of points on the inner circle (white coating) and the ones on the outer ring (black coating). Figure 5a illustrates the lidar points fallen on a target circle in top view; the four crosses in the middle are lidar points in the inner circle with white coating, and the stars denote the points on the outer black ring. Figure 5b shows the same points in side view; to better illustrate the elevation difference, the average elevations of the inner circle points and the outer ring points are shown by two horizontal lines.

Once the lidar target positions have been determined from the dataset, their coordinates are compared to the surveyed values. Tables 3a and 3b contain the errors in the three coordinate directions at the target locations in strip #1

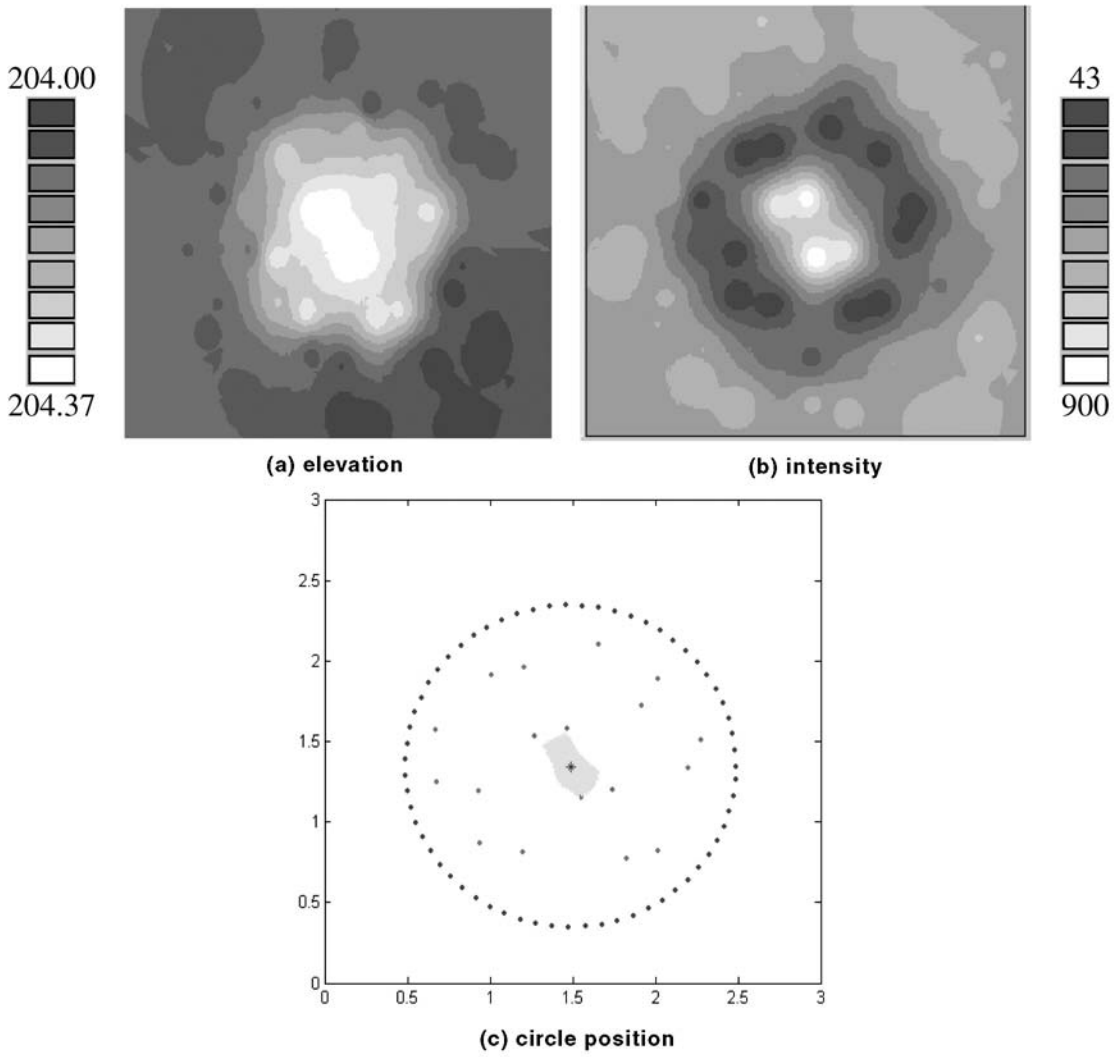

Figure 4. Target in elevation (a), and intensity data (b), and identified target circle (c). A color version of this figure is available on the ASPRS website: **www.asprs.org**.

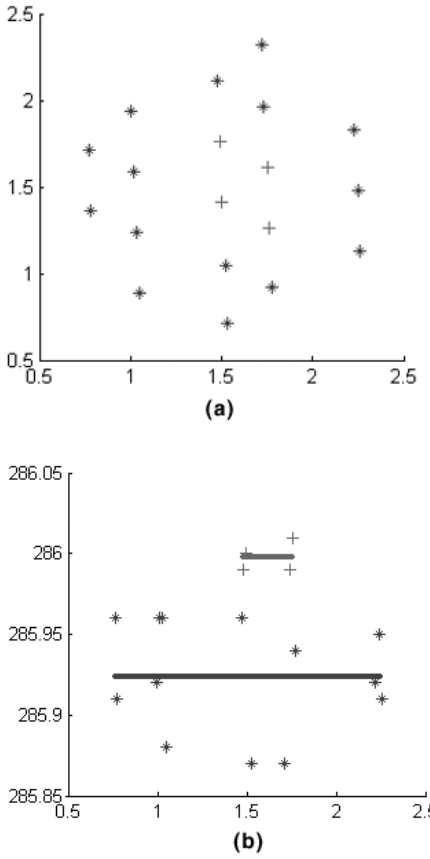

Figure 5. Effect of reflectivity on range measurements: (a) lidar points on target in top view, and (b) in side view.

and strip #2, respectively. The errors are the differences between the computed target coordinates from the lidar strip and their GPS-measured coordinates that had a horizontal and vertical accuracy of approximately 2 cm and 3 cm, respectively. The standard deviation of the computed lidar target center locations shown in Table 3 are provided by the target identification algorithm. The horizontal position determination accuracies for all targets are within 10 cm; that is in good correspondence with our earlier simulation results (see Table 1). In a sense, these values can be considered as an absolute measure, as the horizontal accuracy of the GPS-surveyed coordinates is almost negligible compared to them. The elevation accuracy of the determined target position is calculated based on the standard deviation of the vertical coordinate of the lidar points and the number of points falling on the target.

The detected differences in Table 3 clearly show a vertical shift in both strips. In general, the target coordinates fall below their GPS-determined elevations in both strips. In the case of strip #2, the vertical shift is even more significant, about 14 cm. The determined horizontal errors, however, are not significant for most of the targets; they fall below their determined standard deviation values, except for one or two targets. The detected errors show that the lidar data is of good quality, but by using targets the accuracy can be improved, especially the vertical accuracy, where a noticeable shift was detected.

After analyzing the results, a three-dimensional similarity transformation, applied separately for both strips including all the targets, was found to be adequate for the correction. The last three columns of Table 3a and 3b list the residual errors in three-dimensions at the targets after the transformation was applied to strip #1 and #2, respectively. As expected, the horizontal coordinates did not change much at the targets where the detected differences were originally in the range of the horizontal coordinate determination accuracy. However, at few targets where the determined errors were significant, an improvement was found. The transformation significantly decreased the vertical differences, and they are approximately in the range of the vertical accuracy of the determined target coordinates.

The goal of applying the specifically designed lidar targets in transportation corridor mapping was to improve the overall accuracy of the lidar data and to achieve the most accurate road surface data possible. Since the test area was a busy freeway, ground truth measurement of the road surface was not

TABLE 3. ERRORS AT TARGET LOCATIONS WITH THEIR STANDARD DEVIATIONS AND RESIDUALS AFTER APPLYING 3D SIMILARITY TRANSFORMATION TO STRIP #1 (A) AND STRIP #2 (B)

	Error [m]			Standard Deviation [m]			Residual [m]		
Target ID	Easting	Northing	Elevation	Easting	Northing	Elevation	Easting	Northing	Elevation
A									
307	−0.01	0.03	−0.18	0.07	0.07	0.02	−0.05	0.03	−0.03
108	0.05	−0.06	−0.06	0.06	0.08	0.02	0.02	−0.04	0.04
308	0.05	−0.03	−0.07	0.08	0.05	0.02	0.02	−0.01	0.01
109	0.13	0.00	−0.05	0.06	0.08	0.02	0.10	0.03	0.02
309	−0.02	0.00	−0.08	0.08	0.07	0.02	−0.04	0.03	−0.02
110	0.00	0.07	−0.05	0.04	0.05	0.02	−0.02	0.11	0.00
310	0.01	−0.13	−0.06	0.04	0.05	0.02	−0.01	−0.08	−0.02
Mean	0.03	−0.02	−0.08				0.00	0.01	0.00
Std	0.05	0.06	0.05				0.05	0.06	0.03
B									
107	0.04	0.10	−0.11	0.03	0.05	0.02	0.04	0.03	−0.01
108	0.01	−0.03	−0.13	0.04	0.05	0.02	0.01	−0.10	0.02
109	−0.05	0.07	−0.16	0.02	0.01	0.03	−0.05	0.00	−0.02
110	0.10	−0.02	−0.12	0.03	0.04	0.02	0.10	−0.09	0.01
310	−0.02	0.18	−0.17	0.06	0.05	0.02	−0.01	0.11	−0.01
Mean	−0.02	0.06	−0.14				0.02	−0.01	0.00
Std	0.06	0.09	0.03				0.06	0.09	0.02

TABLE 4. ELEVATION DIFFERENCES BETWEEN STRIP#1 AND STRIP#2 BEFORE AND AFTER TRANSFORMATION

	Elevation Difference [m]	
Road Area	Before	After
#1	−0.13	−0.04
#2	−0.14	−0.05

feasible, as it would have been dangerous for the survey crew, and therefore, to assess the achieved accuracy improvement, the elevation differences between the road surface patches in the two overlapping strips were checked before and after the target-based correction (three-dimensional similarity transformation) of both strips. Two 5 m by 5 m road surface areas were selected from the overlapping area of the two strips; one was in the vicinity of target #109 (denoted Area #1) and the other one was halfway between target #110 and #310 (denoted Area #2). Table 4 shows the elevation differences between the two strips at the selected two road areas before and after applying the similarity transformation to the lidar strips separately. The elevation difference was determined by fitting a plane to the data. As illustrated by Table 4, applying the transformation based on the lidar targets, the achieved road surface extraction accuracy improvement is significant. For both road surface areas, a similar magnitude of improvement was found; the original 13 to 14 cm elevation difference of the road surfaces in the two strips decreased to the 4 to 5 cm level, which is in the range of the combined error budget of the control determination accuracy and the laser ranging error.

Test Flight 2

The second performance validation experience was a dedicated flight for testing the targets at different lidar point densities, different pulse rates, scan frequency, scan angle settings, and the consistency of the errors in the lidar strips. The test area was located in Madison County, Ohio; a 7 km long section of US Route 40 was flown in both directions with a couple of cross strips. The flight parameters are shown in Table 5. Both elevation and intensity data were collected to facilitate lidar target identification in the data. For this test flight, again 15 pairs of lidar targets were placed symmetrically along the two sides of the road. However, to facilitate more extensive analysis, the targets were placed much denser than in the case of the first test flight. With varying distance from each other, targets in the middle had an average spacing of 130 m, towards the end of the strips 500 m, and at the end 950 m, respectively. Figure 6 illustrates the lidar target locations in the measured strips. The origins of the target circles were GPS-surveyed at a horizontal coordinate accuracy within 2 cm, while the vertical accuracy was about 3 cm.

To check the quality of the data, all the strips were automatically processed using the developed software. Figure 7 illustrates a 3 m by 3 m area around a lidar target (target # 201) in three overlapping strips in elevation data

TABLE 5. MADISON TEST FLIGHT PARAMETERS

Altitude (AGL)	~700 m
Scan Angle	10°, 20°
Pulse Rate	33, 50, 70 kHz
Scan Frequency	36–70 Hz
Point Density	Varying depending on settings
Footprint Size	21 cm

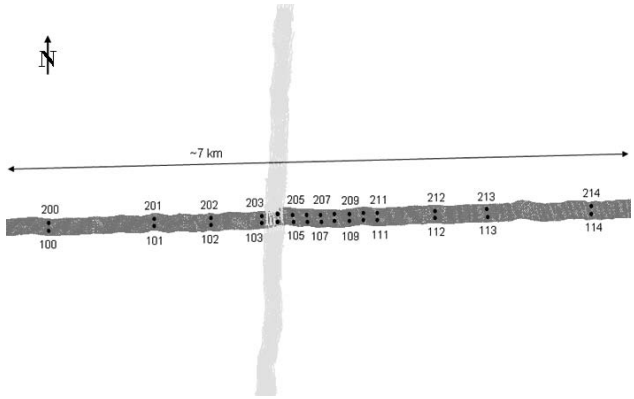

Figure 6. Lidar strips with target locations from test area 2. A color version of this figure is available on the ASPRS website: **www.asprs.org**.

(Figure 7a) and intensity data (Figure 7b). The three strips were flown with different lidar settings, and therefore have different point densities. The first figure shows the target in a strip flown with 70 kHz pulse rate, 70 Hz scan frequency, and 10 degrees scan angle; the second with 50 kHz pulse rate, 44 Hz scan frequency, and 20 degrees scan angle; and the lidar settings for the third strip were 33 kHz pulse rate, 51 Hz scan frequency, and 10 degrees scan angle. For visualization purposes, the lidar points are interpolated and the figures are shown in gray scale based on the elevation and intensity values. In spite of the interpolation, the locations of the lidar points are visible. Due to the different settings, in the first strip about 20 points, while in the second and third strips about 10 lidar points fell on the target. Carefully comparing the three elevation figures, an elevation difference between the strips is clearly visible. The intensity information clearly separates the inner target circle points and the outer target ring points; the difference between the three different intensity images of the same target illustrates the relative nature of intensity data.

As an example, Table 6 shows the errors with their standard deviation values in the three coordinate directions at the target locations for a typical strip. The horizontal and vertical components of the errors are visualized in Plate 2a and 2c, respectively (different exaggeration was applied for the two components; the radius of the circles in Plate 2c represents the vertical error magnitude). The strip was flown with 70 kHz pulse rate, 70 Hz scan frequency, and 10 scan angle, and all of the 30 targets were successfully identified and accepted by the developed software. Although there is a noticeable common shift in Plate 2a, the determined horizontal position errors cannot be considered significant as for most of the targets they are within their standard deviation values. However, there is a significant vertical shift, which is consistent for all the targets; they appear to be about 20 cm lower in the lidar data than their GPS-measured coordinates. After analyzing these errors, it is difficult to conclude that there is no horizontal error, as there could be an error less than 10 cm horizontally (as suggested in Plate 2a), but due to the horizontal positioning limitations, it cannot be reliably detected; any vertical error larger than 2 to 3 cm can be detected using the targets.

The three-dimensional similarity transformation applied to the strip was found to be adequate to correct for the errors found in this lidar strip. The last three columns of Table 6 illustrate the residual coordinate errors after the transforma-

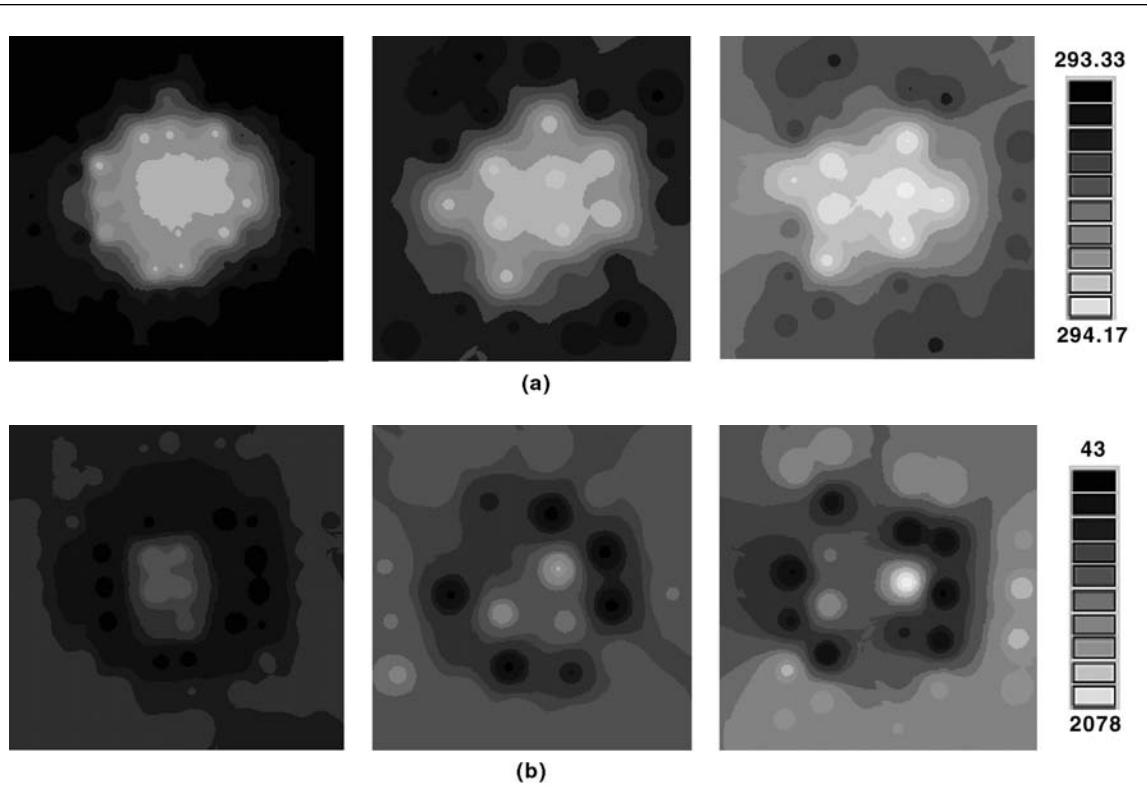

Figure 7. Lidar target in three overlapping lidar strips: (a) elevation and (b) intensity data.

TABLE 6. ERRORS AT TARGET LOCATIONS WITH THEIR STANDARD DEVIATIONS AND RESIDUALS AFTER APPLYING 3D SIMILARITY TRANSFORMATION

	Error [m]			Standard Deviation [m]			Residual [m]		
Target ID	Easting	Northing	Elevation	Easting	Northing	Elevation	Easting	Northing	Elevation
100	0.09	−0.03	−0.22	0.08	0.06	0.02	0.03	0.00	−0.01
200	0.11	0.10	−0.18	0.07	0.08	0.02	0.05	0.12	0.03
101	0.14	0.00	−0.20	0.06	0.04	0.02	0.08	0.01	0.01
201	−0.05	0.02	−0.19	0.06	0.08	0.02	−0.11	0.02	0.01
102	0.05	0.00	−0.20	0.08	0.06	0.02	−0.01	0.00	0.01
202	0.06	0.02	−0.20	0.05	0.05	0.02	0.00	0.02	0.01
103	0.10	−0.02	−0.20	0.03	0.08	0.02	0.03	−0.04	0.01
203	0.08	0.01	−0.19	0.07	0.04	0.03	0.01	−0.01	0.01
104	0.14	0.00	−0.22	0.06	0.04	0.02	0.08	−0.02	−0.01
204	0.03	0.08	−0.22	0.07	0.07	0.02	−0.03	0.06	−0.02
105	0.19	−0.02	−0.19	0.08	0.05	0.02	0.13	−0.04	0.01
205	0.03	−0.04	−0.21	0.07	0.04	0.02	−0.03	−0.06	−0.01
106	0.07	0.01	−0.20	0.03	0.04	0.02	0.01	−0.01	0.01
206	0.03	0.10	−0.20	0.03	0.08	0.02	−0.03	0.07	−0.01
107	0.07	−0.03	−0.23	0.09	0.08	0.02	0.01	−0.05	−0.02
207	0.01	0.06	−0.20	0.03	0.03	0.02	−0.05	0.04	0.00
108	0.11	−0.03	−0.19	0.06	0.06	0.02	0.05	−0.06	0.02
208	0.00	0.07	−0.22	0.07	0.08	0.02	−0.07	0.04	−0.02
109	0.11	−0.02	−0.22	0.07	0.09	0.03	0.04	−0.05	−0.02
209	0.09	0.09	−0.21	0.05	0.09	0.02	0.02	0.05	−0.01
110	0.03	−0.03	−0.21	0.06	0.05	0.02	−0.03	−0.06	−0.01
210	0.07	0.05	−0.21	0.09	0.06	0.02	0.01	0.01	−0.01
111	0.15	0.00	−0.23	0.08	0.06	0.02	0.09	−0.04	−0.03
211	0.03	0.04	−0.20	0.05	0.07	0.02	−0.03	0.00	0.00
112	0.06	−0.03	−0.21	0.06	0.09	0.02	0.00	−0.07	−0.01
212	0.02	0.07	−0.18	0.03	0.05	0.02	−0.04	0.02	0.01
113	0.15	0.01	−0.19	0.08	0.09	0.03	0.08	−0.05	0.01
213	0.06	0.10	−0.19	0.04	0.04	0.03	0.00	0.04	0.01
114	0.20	0.01	−0.15	0.07	0.10	0.02	0.13	−0.07	0.04
214	0.10	0.16	−0.19	0.07	0.08	0.02	0.04	0.09	0.00
Mean	0.08	0.03	−0.20				0.02	0.00	0.00
Std	0.06	0.05	0.02				0.06	0.05	0.02

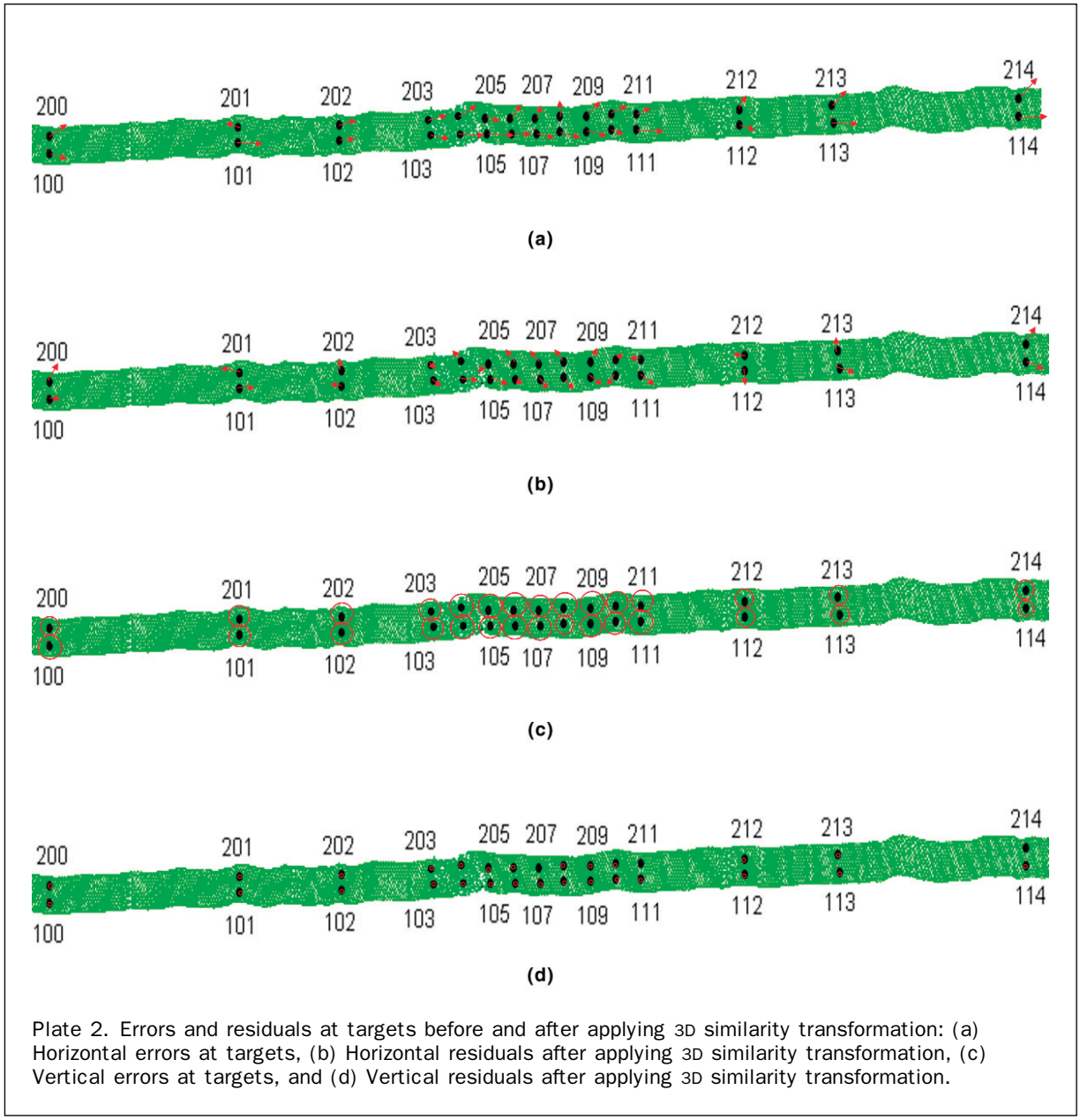

Plate 2. Errors and residuals at targets before and after applying 3D similarity transformation: (a) Horizontal errors at targets, (b) Horizontal residuals after applying 3D similarity transformation, (c) Vertical errors at targets, and (d) Vertical residuals after applying 3D similarity transformation.

tion, visualized in Plate 2b and 2d. The horizontal errors changed only in terms that the common shift was eliminated, and the magnitude was reduced after the transformation. However, the vertical errors changed significantly; their mean value decreased to zero, and the standard deviation corresponds to the vertical target position determination accuracy.

Table 6 illustrates a typical strip. All strips were similarly processed, and the data, in general, were found to be of good quality. Nevertheless, a few centimeters of vertical shift was detected in all strips and was corrected. Within each strip the errors at the different target locations were found to be consistent. Table 7 provides a summary of the errors found in the different lidar strips and shows the mean vertical errors found at the target locations for the different strips together with their standard deviations. Table 7 also shows the actual lidar settings for the strips, pulse rate, scan frequency, scan angle, point density, and the number of targets found in each strip. It should be mentioned here that those strips containing only 2 to 4 targets were cross strips as illustrated in Figure 6. Note the relationship between the pulse rate and the found vertical error. The assessment of achievable accuracy of lidar systems, in general, is a difficult task, as besides navigation and sensor calibration errors, the error budget is influenced by several other factors such as laser pulse energy level, beam divergence, pulse rate, scan mechanism, and time synchronization. Further discussions could analyze the effect of those parameters on the achievable accuracy using lidar-specific ground targets.

Discussion

The two test flights conducted at different locations and in different seasons produced similar results. In both cases, the horizontal errors at the lidar targets were within their expected accuracy range defined by the footprint size of the

TABLE 7. MEAN VERTICAL TARGET ELEVATION ERRORS IN THE DIFFERENT MADISON STRIPS

Strip ID	PRF [kHz]	Scan Freq [Hz]	Scan Angle [deg]	Point Density [pts/m^2]	Mean Target Elevation Difference [m]	Std Elevation Difference [m]	Number of Targets in Strip
4	70	70	10	7.7	−0.20	0.02	30
2b	70	70	10	7.7	−0.20	0.02	30
4b	70	70	10	7.9	−0.11	0.01	29
5b	70	70	10	8.9	−0.13	N/A	2
8b	70	70	10	7.2	−0.15	N/A	2
7	70	50	20	4.2	−0.12	0.02	29
8	70	50	20	4.2	−0.12	0.01	25
15	70	50	20	3.7	−0.11	0.03	3
19	70	50	20	4.7	−0.13	0.02	4
				Mean	−0.14		
				Std	−0.04		
11	50	63	10	5.6	−0.10	0.02	28
18	50	63	10	5.8	−0.10	N/A	2
10	50	44	20	3.2	−0.12	0.02	19
13	50	44	20	3.0	−0.10	0.02	22
14	50	44	20	3.0	−0.07	0.02	20
17	50	44	20	2.8	−0.08	N/A	2
				Mean	−0.10		
				Std	0.02		
2	33	51	10	3.8	−0.05	0.02	23
5	33	51	10	3.4	−0.03	0.02	19
12	33	51	10	4.3	0.00	0.02	27
9	33	36	20	1.8	−0.06	0.01	11
				Mean	−0.04		
				Std	0.03		

laser pulse and the horizontal component of the navigation solution. In several strips, there was a tendency of a small, but noticeable, shift in a common direction. The vertical errors, in contrast, exhibited a typical pattern of all the vertical lidar point coordinates falling below the surveyed target elevations.

There were three transformation models tested in our investigation; results are shown only for the three-dimensional similarity transformation case. The simplest model, using a common vertical shift, produced acceptable results in most cases. The similarity transformation, however, consistently delivered good results by not only eliminating the vertical shift, but by reducing the horizontal errors in several cases. However, judging the horizontal errors is rather difficult as the target position determination accuracy in the horizontal component is almost an order below the vertical one; the horizontal target position determination accuracy is more dependent on the laser pulse footprint size and the number of points falling on the target. Applying a 12-parameter three-dimensional affine transformation produced comparable results for test 2, where the number of targets was large. For a smaller number of targets, however, the fit at targets was good but a noticeable warping of the strip was observed.

Conclusions

This paper proposed the use of ground control targets specifically designed for lidar data to provide quality control for applications that require centimeter-level, engineering scale mapping accuracy. Extensive simulations were performed to determine the most favorable lidar target design. Results confirmed that the optimal target is rotation invariant, circular-shaped, elevated from the ground and a 1 m circle radius can provide sufficient accuracy from a point density of about 5 pts/m^2. Targets larger than 2 m in diameter will not lead to significant improvements. In addition, the two-concentric-circle design (the inner circle has one-half the radius of the outer circle) with different coatings produced considerable accuracy improvements in the horizontal position.

The test results obtained from two flights show that the specifically designed lidar targets can improve or validate centimeter-level accuracy of the final lidar product for applications that require engineering scale mapping accuracy. The target processing is automated, and the developed software toolbox provides robust processing and is ready for normal map production. The algorithms developed to determine target coordinates in lidar data can provide 5 to 10 cm horizontal positioning accuracy (at 25 cm footprint size) and 2 to 3 cm vertical accuracy of the target coordinates at 5 pts/m^2 lidar point density. Consequently, larger than 10 cm horizontal errors and vertical errors larger than 2 to 3 cm in the lidar data can be detected and corrected using the lidar targets.

Our investigation was primarily concerned with highway corridor mapping. However, the results can be extended to other applications as long as the impact of the landscape type is not significant. For example, highly built-up urban areas or areas with no or limited vegetation could also benefit from using lidar-specific targets when high accuracy is required.

Acknowledgments

The authors would like to thank the Ohio Department of Transportation for funding this research, manufacturing the lidar targets, and flying lidar surveys to acquire essential data for this research. A special thank is due to John Ray,

Administrator of Office of Aerial Engineering and Joe Tack for providing assistance in the data preparation.

References

Baltsavias, E.P., 1999. Airborne laser scanning: basic relations and formulas, *ISPRS Journal of Photogrammetry and Remote Sensing*, 54:199–214.

Behan, A., 2000. On the matching accuracy of rasterized scanning laser altimeter data, *International Archives of Photogrammetry and Remote Sensing*, 33 (Part 2B):75–82.

Burman, H., 2002. Laser strip adjustment for data calibration and verification, *International Archives of Photogrammetry and Remote Sensing*, 34(Part 3A):67–72.

Crombaghs, M.J.E., R. Brügelmann, and E.J. de Min, 2000. On the adjustment of overlapping strips of laser altimeter height data, *International Archives of Photogrammetry and Remote Sensing*, 33 (Part B3/1):224–231.

Csanyi, N., C. Toth, D. Grejner-Brzezinska, and J. Ray, 2005. Improving LiDAR data accuracy using LiDAR-specific ground targets, *Proceedings of the ASPRS Annual Conference*, Baltimore, Maryland, 07–11 March, unpaginated CD-ROM.

Csanyi, N., and C. Toth, 2004. On using LiDAR-specific ground targets, *Proceedings of the ASPRS Annual Conference*, Denver, Colorado, 23–28 May, unpaginated CD-ROM.

Duda, R.O., and P.E. Hart, 1972. Use of the Hough Transformation to detect lines and curves in pictures, *Graphics and Image Processing*, 15:11–15.

Filin, S., 2003. Analysis and implementation of a laser strip adjustment model, *International Archives of Photogrammetry and Remote Sensing*, 34(Part 3/W13):65–70.

Hough, P.V.C., 1959. Machine analysis of bubble chamber pictures, *Proceedings of the International Conference on High Energy Accelerators and Instrumentation*, CERN.

Hough, P.V.C., 1962. *Methods and Means for Recognizing Complex Patterns*, U.S. Patent 3069654.

Kager, H., and K. Kraus, 2001. Height discrepancies between overlapping laser scanner strips, *Proceedings of Optical 3D Measurement Techniques V*, October, Vienna, Austria, pp. 103–110.

Kilian, J., N. Haala, and M. Englich, 1996. Capture and evaluation of airborne laser scanner data, *International Archives of Photogrammetry and Remote Sensing*, 31(Part B3):383–388.

Maas, H.-G., 2000. Least squares matching with airborne laser-scanning data in a TIN structure, *International Archives of Photogrammetry and Remote Sensing*, 33(Part B3/1): 548–555.

Maas, H.-G., 2001. On the use of pulse reflectance data for laser-scanner strip adjustment, *International Archives of Photogrammetry, Remote Sensing and Spatial Information Sciences*, 33(Part 3/W4):53–56.

Renslow, M., 2005. The status of lidar today and future directions, *Proceedings of the 3D Mapping from InSAR and Lidar Workshop*, ISPRS WG I/2, Banff, Canada, June 07–10, unpaginated CD-ROM.

Toth, C., N. Csanyi, and D. Grejner-Brzezinska, 2002. Automating the calibration of airborne multisensor imaging systems, *Proceedings of the ACSM-ASPRS Annual Conference*, Washington, D.C., 19–26 April, unpaginated CD ROM.

Toth, C. 2004. Future trends in lidar, *Proceedings of the ASPRS 2004 Annual Conference*, Denver, Colorado, 23–28 May, unpaginated CD-ROM.

Vosselman, G., and H.-G. Maas, 2001. Adjustment and filtering of raw laser altimetry data, *Proceedings of the OEEPE Workshop on Airborne Laserscanning and Interferometric SAR for Detailed Elevation Models*, OEEPE Publications No. 40, pp. 62–72.

Vosselman, G., 2002. On the estimation of planimetric offsets in laser altimetry data, *International Archives of Photogrammetry and Remote Sensing*, 34(Part 3A):375–380.

Vosselman, G., 2002. Strip offset estimation using linear features, *Proceedings of the 3rd International LIDAR Workshop*, 07–09 October, Columbus, Ohio, URL: *http://www.itc.nl/personal/vosselman/papers/vosselman2002.columbus.pdf* (last date accessed: 08 January 2007).